Osmium(II) complexes of 2-[(arylamido)phenylazo]pyridines. New examples of deamination reactions—X-ray structure and redox properties†

Chayan Das,[a] Shie-Ming Peng,[b] Gene-Hsiang Lee[b] and Sreebrata Goswami*[a]

[a] *Department of Inorganic Chemistry, Indian Association for the Cultivation of Science, Kolkata 700 032, India. E-mail: icsg@mahendra.iacs.res.in*
[b] *Department of Chemistry, National Taiwan University, Taipei, Taiwan, Republic of China*

Received (in Montpellier, France) 13th September 2001, Accepted 16th October 2001
First published as an Advance Article on the web

Reaction of $[NH_4]_2[OsBr_6]$ with 2-[(arylamino)phenylazo]pyridine, $NH_4C_5N{=}NC_6H_4N(H)C_6H_4(R)$ [R = H (HL^a) or CH_3 (HL^b)], in the presence of dilute NEt_3 affords multiple products. Five compounds of molecular formulas [Os(HL)(L)Br], **1**, [Os(L)(pap)Br], **2**, two isomers of $[Os(pap)_2Br_2]$, **3** and **5**, and $[Os(HL)(pap)Br_2]$, **4**, where L and pap stand for the conjugate base of HL and 2-(phenylazo)pyridine, respectively, have been separated on a preparative TLC plate. The X-ray structures of the new and representative complexes **1a**, **2a** and **4a** have been solved to characterise them. The complexes **3** and **5** were characterised by comparing their spectral properties with those of the known and analysed samples of isomeric $[Os(pap)_2Br_2]$. Except for complex **1**, the rest are formed due to cleavage of an otherwise unreactive C(phenyl)–N(amine) bond which is promoted by the metal ion. The bidentate-tridentate combination of HL and L in **1** is due to electronic factors. Structural data of the compounds have revealed very strong metal-ligand interactions. Osmium(II)-ligand interactions with the neutral azo ligands, *viz*. HL or pap, are stronger than those with the anionic L ligand. All of the complexes display resolved ^1H NMR spectra. However, the spectral pattern is complex due to serious overlap of the resonances. There are multiple electronic transitions in the range 1200–220 nm. The lowest energy transition (HOMO → LUMO) is presumably due to metal-to-ligand charge transfer (MLCT). These complexes undergo multiple and successive one-electron redox processes. The lowest potential anodic response, in each case, has been assigned to the Os^{II}/Os^{III} couple. $E_{1/2}$ of this response in **1** and **2** is similar and occurs near 0.45 V. Low oxidation potentials of the above couples allowed the generation of $[\mathbf{1a}]^+$ and $[\mathbf{2a}]^+$ in solution by exhaustive constant potential coulometry. The trivalent osmium complexes showed rhombic EPR spectra at 77 K. Distortion parameters using the observed g values have been computed.

The coordination chemistry of the anionic tridentate N_3 ligand, 2-[(arylamido)phenylazo]pyridine, L of 3d metal ions has been rich and versatile.[1,2] Its conjugate acid[1–5] HL is obtained by a cobalt promoted amination reaction[1,2,4,5] at coordinated 2-(phenylazo)pyridine [pap]. The compound HL readily loses an H^+ (pK_a 8.5) (Scheme 1) and the anion L coordinates to metal in a bischelating tridentate fashion. The (phenylazo)pyridine part of L is soft[6] and is capable of stabilising low oxidation states of metal ions, while the strong electron donor amido part prefers high valent metal ions. The tunable donor-acceptor properties of the chromophores in L help in stabilisation of the metal ions in variable valence states. Thus, the iron compound $[Fe(L)_2]^{n+}$ is known[1] to exist both as $[Fe^{III}(L)_2]^+$ ($n = 1$) and $[Fe^{II}(L)_2]$ ($n = 0$). Another interesting feature of this ligand is that it stabilises the uncommon low-spin states of metal ions. Amongst these, the low-spin complex $[Mn(L)_2]$ deserves special mention.[2] Extensive delocalisation in the present anionic ligand along its backbone is responsible for many of the uncommon properties of the complexes of L.

Our current interest[7] in the chemistry of heavier metal ions involving redox non-innocent ligands persuaded us to explore the osmium chemistry of HL. Osmium being kinetically inert, different mixed ligand species were anticipated. Unlike the 3d metal ion chemistry of L, described above, the osmium chemistry with HL is not straight forward. The metal ion here promotes cleavage of an otherwise unreactive C(phenyl)–N(amine) single bond,[8] leading to deamination of the ligand.

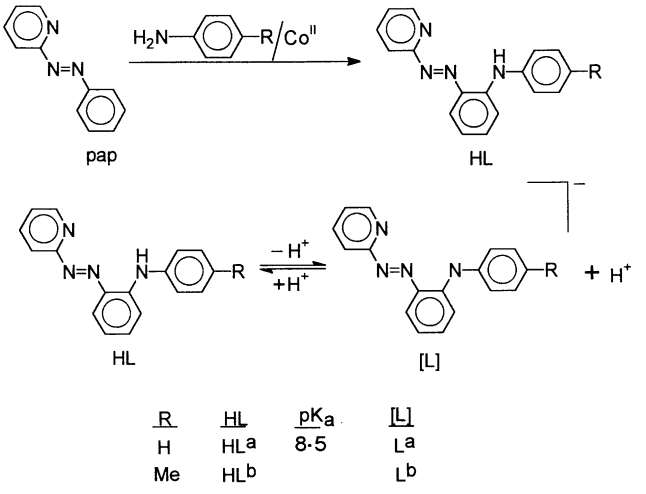

Scheme 1

† Electronic supplementary information (ESI) available: partial energy level diagrams and molecular orbitals of **1a**, **2a** and **4a**, UV-vis spectra of 4 complexes and cyclic voltammograms of **1b**, **2b** and **4b**. See http://www.rsc.org/suppdata/nj/b1/b108507g/

 DOI: 10.1039/b108507g

Herein we report the isolation and characterisation of the multiple products that are obtained from a single reaction of $[NH_4]_2[OsBr_6]$ with HL. Single crystal X-ray structure analyses of the complexes are used for their authentication.

Results and discussion

Synthesis and structural characterisation

The 1 : 2 reaction of $[NH_4]_2[OsBr_6]$ with HL in boiling methanol in the presence of dilute NEt_3 produced a brown solution in about 5 h. The crude mass, so formed, was a mixture of several products. Five pure compounds were successfully separated from the crude mass on a preparative TLC plate (Scheme 2). Except the first brown compound, **1**, the rest (**2**–**5**) were formed due to deamination of the ligand HL. Notably, this reaction is solvent dependent. For example, it does not proceed at all in other solvents like ethanol, *t*-butanol, 2-methoxyethanol, *etc.*

Brown (I), 1. A brown band was first eluted with benzene. The compound, **1**, was obtained by evaporation of the benzene eluate in *ca.* 20% yield. The compound, **1a** ($HL = HL^a$), formed suitable X-ray quality crystals for structure determination.

Fig. 1 shows the ORTEP and atom numbering scheme for **1a**. In this complex, the central osmium(II) is surrounded by a distorted octahedral N_5Br coordination environment. One of the two extended ligands, L^a, is monoanionic, tridentate and chelates to osmium through N(5), N(7) and N(8) with deprotonation of the amine nitrogen. The second ligand, HL^a, on the other hand, is neutral and chelates to the metal ion only through the pyridine nitrogen N(1) and the azo nitrogen N(3). The amine nitrogen atom N(4) of this ligand bears a hydrogen and remains pendant. The sixth position is occupied by a Br ion forming a hexacoordinated compound of formula $[Os(HL^a)(L^a)Br]$. The presence of a hydrogen at N(4) is confirmed based on its ^1H NMR spectrum (*vide infra*). It may be recalled here that in all its known complexes with 3d metal ions the ligand HL loses a proton spontaneously and binds as an anionic tridentate donor to yield metal complexes[1,2] of general formula $[ML_2]^{n+}$. Notably, the relative geometry of the coordinating atoms in **1** are different than those in $[ML_2]^{n+}$ complexes. The orientations within the pairs of pyridyl-N, azo-N and amido-N atoms in $[ML_2]^{n+}$ complexes are *cis*, *trans* and *cis*, respectively. In contrast, the geometry with respect to the pairs of pyridyl-N and azo-N in the osmium complex **1** is *cis*, *cis* (Scheme 3). In this orientation, the azo-N of the protonated HL is *trans* to the coordinated Br. It implies that the amine N(4) is far from the sixth coordination site and hence remains protonated and uncoordinated. The relatively preferred *cis*, *cis* orientation in osmium(II) is due to electronic factors. Unlike the 3d metal ions, the Os(II) ($5d^6$) ion is known to enter into π-interactions very effectively with the ligand π* orbitals. Thus, very strong dπ-azo(π*) back-bonding is a persistent feature of M-pap chelates. In the *trans*-N(azo), N(azo) pair orientation, the π*(azo) orbitals compete for the same metal dπ orbital, which is expected to weaken back-bonding. In fact, such a *trans* orientation has never been observed[9,10] in $[M(pap)_2Cl_2]$ ($M = Ru$, Os). Therefore, the tridentate and bidentate coordination modes of L and HL in [Os(HL)(L)Br] are understandable.

The bond distances in the osmium compound under consideration indicate considerable metal-ligand interactions. The N–N length [N(2)–N(3), 1.336(3) Å] is appreciably elongated compared to that observed[11] in $[papH]ClO_4$. This is due to considerable Os–HL π-bonding with major involvement of the azo functionality. The shortest Os–N length (1.946 Å) in this complex is the bond between Os and N(3) of neutral HL^a, which further confirms the existence of strong Os–azo π bonding. The main features of bonding of the anionic tridentate $[L^a]$ are similar to those observed[1,2] in other M–L complexes. Extensive electron delocalisation along the ligand backbone has been noted. For the same reason the Os–N(7) bond is short and comparable to the Os–N(3) bond length, but is appreciably shorter than the three other Os–N bonds in the same molecule.

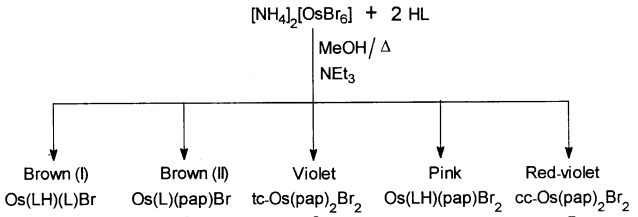

Scheme 2

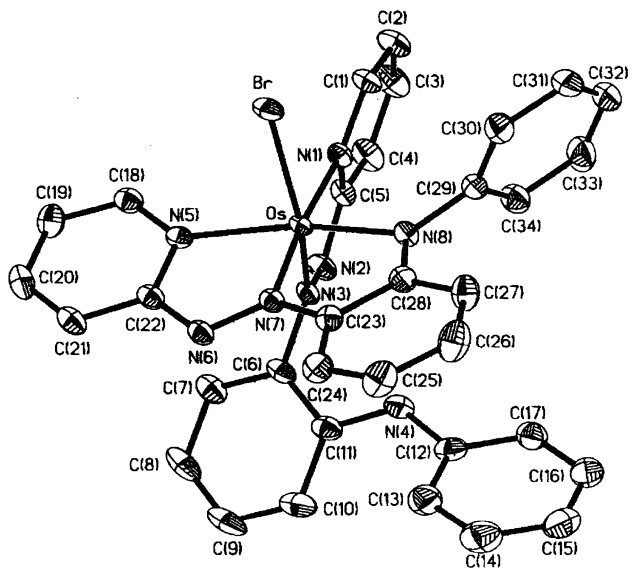

Fig. 1 Molecular structure and atom numbering scheme for $[Os(HL^a)(L^a)Br]$, **1a.** Selected bond lengths (Å): Os–N(1) 2.074(2), Os–N(3) 1.946(2), Os–N(5) 2.088(2), Os–N(7) 1.953(2), Os–N(8) 2.031(2), Os–Br 2.5301(3), N(2)–N(3) 1.336(3), N(6)–N(7) 1.319(3), N(7)–C(23) 1.386(3), N(8)–C(28) 1.369(4), N(8)–C(29) 1.440(4).

Brown (II), 2. The second brown band, which overlapped with the first brown band, was also eluted with benzene. Evaporation of benzene solution yielded the brown (II) com-

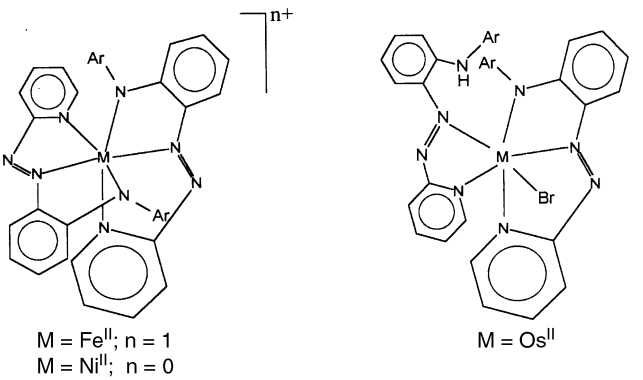

Scheme 3

pound in *ca.* 20% yield. The colour and the physical properties of this compound are similar to those of compound **1**. The compound **2a** (HL = HL[a]) also formed suitable X-ray quality crystals for structure determination. Fig. 2 shows the ORTEP and atom numbering scheme for **2a**. Analysis of the crystal data indeed authenticated the formation of a mixed ligand compound, [Os(L)(pap)Br], from the reaction as shown in Scheme 2. One of the two HL ligands here has undergone a deamination reaction with cleavage of a C–N bond to form a bidentate neutral 2-(phenylazo)pyridine (pap) ligand. Compounds **1** and **2** are similar with the exception that in **1** an ortho-substituted ligand, HL, replaces the pap ligand. The important bond distances in **2a** and **1a** are collected in the respective figure captions, which indeed showed structural similarities between the two compounds.

Violet, 3. Working up of the eluate followed by crystallisation of the third violet band yielded the known[12] *trans*, *cis*-$Os(pap)_2Br_2$. Thus, compound **3** has formed due to complete deamination of HL.

Pink, 4. A pink band moved after the above violet band, the yield of which was *ca.* 10%. By repeated trials we were able to grow suitable X-ray quality crystals of **4a**. The ORTEP and atom numbering scheme of the compound are shown in Fig. 3. In this compound there are two types of chelating ligands. One of the extended ligands is HL[a], which acts as a bidentate chelate as in **1** (*vide supra*) and the second ligand is pap, which is generated due to deamination of HL[a]. There are two cis bromides to complete the hexacoordination of the central osmium(II) in $[Os(HL^a)(pap)Br_2]$. Very strong Os(dπ)-azo(pπ) interactions are the general bonding features in this compound. As a result, the N–N lengths are elongated and Os–N(azo) distances are shorter than Os–N(py) lengths. Selected bond lengths in this compound are collected in the Fig. 3 caption. The relative orientations within the coordinating pairs, N(py), N(py) and N(azo), N(azo), are *cis* and *cis*.

Red-violet, 5. This last red-violet band showed[12] identical spectral properties to those of known *cis*,*cis*-$Os(pap)_2Br_2$. Thus, compounds **3** and **5** are the two isomers of $Os(pap)_2Br_2$ and these are formed due to complete deamination of the ligand HL used in this work.

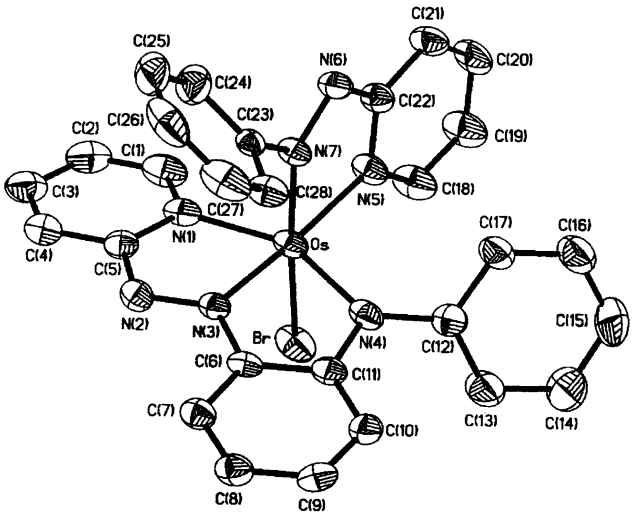

Fig. 2 Molecular structure and atom numbering scheme for [Os(L[a])(pap)Br], **2a.** Selected bond lengths (Å): Os–N(1) 2.079(6), Os–N(3) 1.941(5), Os–N(4) 1.998(6), Os–N(5) 2.084(5), Os–N(7) 1.938(5), Os–Br 2.5321(8), N(2)–N(3) 1.313(7), N(3)–C(6) 1.369(7), N(4)–C(11) 1.395(8), N(4)–C(12) 1.426(9), N(6)–N(7) 1.345(6).

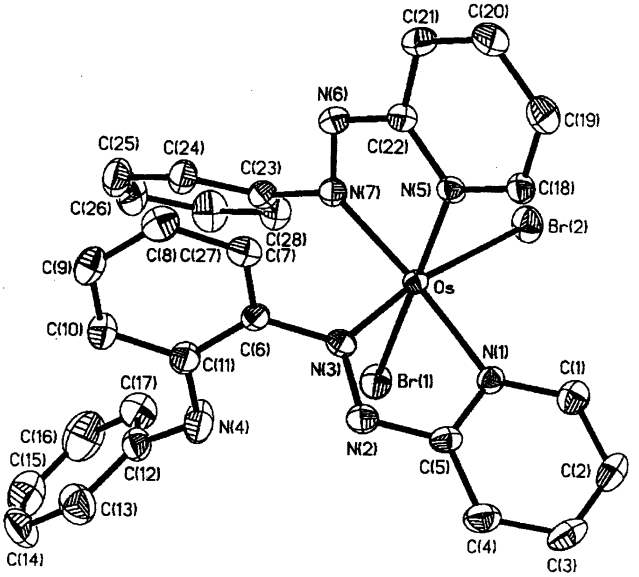

Fig. 3 Molecular structure and atom numbering scheme for [Os(HL[a])(pap)Br_2], **3a.** Selected bond legnths (Å): Os–N(1) 2.086(3), Os–N(3) 1.962(3), Os–N(5) 2.046(3), Os–N(7) 1.990(3), Os–Br(1) 2.5505(4), Os–Br(2) 2.5454(4), N(2)–N(3) 1.311(4), N(6)–N(7) 1.307(5).

Rationale for the deamination reaction. Besides these above five bands there were a few minor overlapping bands, which were observed on the TLC plate. We have not been successful in isolating these in the pure state. Out of the five compounds, four (**2**–**5**) were obtained due to cleavage of at least one C(phenyl)–N(amine) bond. The reaction occurs only in boiling methanol and the mechanism[8] of this bond cleavage could not be established so far. However, the overall reaction may be viewed as hydrogenation of HL across a C–N bond, leading to the formation of pap and Ar–NH_2. We note here that the ligand HL reacts spontaneously with several 3d metal ions, where no such C–N bond cleavage was observed. Moreover, the composition of the metal complex (ML_2^{n+}) involving the 3d elements is different than that observed for the osmium complex. In the osmium complex **1**, one of the two coordinated ligands binds as a neutral bidentate donor with a pendant aryl amine group, which may be responsible for the C–N bond cleavage reaction. It is now known that methanol in the presence of suitable metal complex catalysts can be a useful source of hydrogen for reduction of organic substrates.[13] Oxidative addition of methanol led to the formation of metal complex hydrido intermediates that were shown to be the active species for the hydrogenation reactions. Unfortunately, we have yet to identify any hydrido intermediate from our reaction. Furthermore, we note here that the compounds **1** and **4**, once formed, cannot be converted to **2** and **3** (**5**), respectively, in boiling methanol. Hence it is reasonable that the present deamination reactions occur *via* some transient osmium hydrido intermediates, which were not isolable. Thus, given the obvious limitations in our above proposal, we prefer not to speculate on this point but just to note that it is a possibility.

Spectral properties

There are two notable features in the IR spectra of the osmium complexes: (*i*) the complexes containing bidentate HL systematically showed[14] moderately intense ν_{N-H} in the range 3410–3285 cm^{-1} and (*ii*) the $\nu_{N=N}$ stretching frequencies in the complexes appeared between 1290 and 1220 cm^{-1}, which are appreciably lower[6] than those in the free ligands. These further confirm strong Os(dπ)-azo(pπ) interactions in the present

complexes. The IR spectra contained all other expected vibrations[1,2] due to the coordinated ligands.

The ^{1}H NMR spectra of the complexes were recorded in $CDCl_3$. Except for the violet *trans*, *cis*-Os(pap)$_2$Br$_2$ (**3**) compound, the rest are unsymmetrical and their spectra are complex in nature with a very large number of overlapping proton resonances. However, most of the pyridyl proton resonances appeared in the low field region (δ 9.5–7.3). Notably, the NH resonance in the complexes of HL shifted upfield appreciably. For example, the δ(N–H) of the brown [Os(HL)(L)Br], **1**, appeared near δ 6.00. In comparison, in the free HL this appeared at δ 10.58. The N–H proton in the above complex is shielded by the π-cloud of the phenyl ring of the co-ligand. The two related complexes of [HL^b], [Os(HL^b)(L^b)Br], **1b**, and [Os(L^b)(pap)Br], **2b**, showed two and one methyl resonances, respectively, near δ 2.25 (Fig. 4).

In order to gain some insight into the nature of redox and spectroscopically relevant orbitals, in the new osmium complexes, standard extended Hückel MO calculations using the crystallographic parameters were performed for **1a**, **2a** and **4a** using the semi-empirical CACAO programme by Mealli and Proserpio.[15] The MOs of the complexes have some common features: (*i*) the HOMO is primarily a metal orbital where the ligand contribution is <10%, (*ii*) the two closely spaced molecular orbitals LUMO and LUMO + 1 are strongly delocalised. These have *ca.* 35–40% metal d-character with significant contributions from the ligand π-acceptor (–N=N–) orbitals, and (*iii*) the filled HOMO-1 is also delocalised, where the metal contribution is a little over 25%. Partial energy level diagrams of the representative complexes **1a**, **2a** and **4a**, along with a pictorial presentation of the representative MOs, are submitted as ESI (Fig. S1–S6).

The complexes **1**, **2** and **4** displayed multiple bands and shoulders in the region 250–1400 nm in dichloromethane solution (Table 1). Notably, spectral patterns of the complexes **1** and **2** are similar but are complex in nature with a large number of transitions.[16] The spectrum of **4**, on the other hand, is relatively simpler. For example, each of **1** and **2** displays four transitions in the visible range while the complex **4** shows only one intense transition near 515 nm and a broad band near 820 nm, which is similar[12] to what is observed for *cc*-Os(pap)$_2$Br$_2$. We note here that the two coordinated organic ligands in the former two complexes **1** and **2** are totally different. In contrast, the two ligands in **3**, though not identical are similar. The ligand HL may be viewed as a substituted pap ligand with a–N(H)Ar substituted on the ortho carbon of the phenyl ring of pap. This ortho-substitution appears to have very little electronic effects and hence the physicochemical properties of the complexes of HL and those of metal-pap complexes are similar. The lowest energy transitions in the present complexes are broad ($\varepsilon > 1000$ M^{-1} cm^{-1}) and are due to nonbonding HOMO → LUMO transitions. Hence these transitions are formally metal-to-ligand charge transfer (MLCT) transitions.[1,7d] The next higher transitions are more intense and are assigned to transitions between heavily mixed metal-ligand orbitals, LUMO, LUMO+1, HOMO-1 and HOMO-2 orbitals. The UV-range transitions in these complexes are very intense and are assigned to intraligand π-π* transitions. Representative spectra of the complexes are submitted as ESI (Fig. S7).

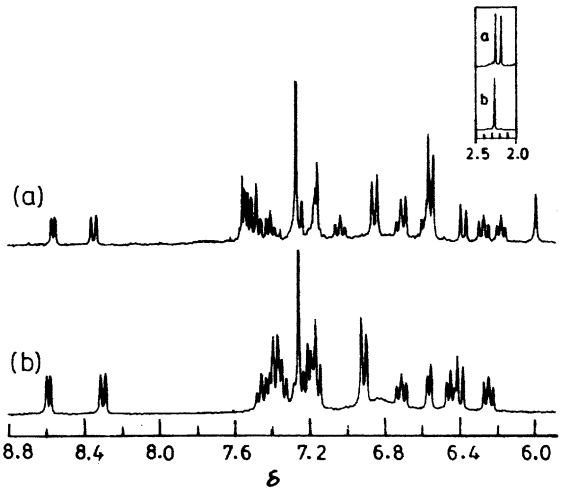

Fig. 4 ^{1}H NMR spectra of (a) [Os(HL^b](L^b)Br] and (b) [Os(L^b)(pap)-Br] in $CDCl_3$. Inset: Resonance due to methyl protons.

Table 1 Electronic spectral data in CH_2Cl_2

Compound	λ_{max}/nm (ε/M^{-1} cm^{-1})
Os(HL^a)(L^a)Br (**1a**)	930(1970)^a, 730(5870), 620(6290), 520(9760)^a, 420(11 620), 290(49 680), 240(42 090)
Os(HL^b)(L^b)Br (**1b**)	890(2300)^a, 730(4390), 620(4630), 490(7310)^a, 420(8600), 290(34200), 230(32000)
Os(L^a)(pap)Br (**2a**)	910(1960)^a, 730(4650)^a, 620(5030)^a, 520(8240)^a, 420(10 120), 360(18 390)^a, 310(26 540), 250(68 090), 230(31 214)
Os(L^b)(pap)Br (**2b**)	920(1770)^a, 730(4700)^a, 620(5190)^a, 520(7870)^a, 420(9870), 310(24 820), 230(28 090)
tc-Os(pap)$_2$Br$_2$ (**3**)	980(900), 580(7980)^a, 525(11 990), 320(27 010)
Os(HL^a)(pap)Br$_2$ (**4a**)	820(1380), 515(11 970), 370(11 960)^a, 290(30 370), 230(31 980)
Os(HL^b)(pap)Br$_2$ (**4b**)	810(1090), 510(9330), 370(10 350)^a, 290(29 640), 230(26 930)
cc-Os(pap)$_2$Br$_2$ (**5**)	850(1200), 518(11 790), 320(17 860), 230(26 160)

^{a} Shoulder.

Redox properties and EPR spectra

Redox properties of the osmium complexes were studied by cyclic voltammetry (CV) with a platinum working electrode. Voltammetric data are collected in Table 2 and representative voltammograms are deposited as ESI (Fig. S8). In all cases dichloromethane was used as solvent. The nature of the voltammograms of the complexes does not change in acetonitrile. However, due to the relatively low solubility of the compounds in acetonitrile, dichloromethane was commonly used for the voltammetric studies. All the potentials are referenced to the SCE (SCE = saturated calomel electrode).

The brown complexes **1** and **2** showed almost identical voltammograms. The complexes exhibited multiple redox responses in the range +1.8 to −1.5 V. There were two electrochemically reversible anodic responses near 0.40 and 0.90 V. The first oxidation in both **1** and **2** occurs from a primarily metal orbital, the HOMO. The second redox active orbital in these complexes is a ligand orbital, HOMO-1. Thus, the second oxidative response may be assigned as ligand oxidation of the amido function. It may be noted here that free HL^a displayed[1] two irreversible anodic responses and a reversible cathodic response at 1.30, 1.00 and −1.15 V, respectively. It is expected that the anodic responses would shift cathodic in the anion L^a. The multiple irreversible cathodic responses in the present complexes are assigned to ligand reductions.

Low potentials for the Os^{II}/Os^{III} couple in the complexes **1** and **2** persuaded us to try and isolate the corresponding osmium(III) complexes [**1**]$^+$ and [**2**]$^+$ in their pure states. Accordingly, we tried to oxidise them both chemically and

Table 2 Electrochemical data in CH_2Cl_2[a]

Compound	Anodic responses[b] $E_{1/2}$/V(ΔE_p/mV) E_{pa}/V	Cathodic responses[b] $E_{1/2}$/V(ΔE_p/mV) E_{pc}/V
1a	0.44(70), 0.91(100), 1.19[c]	−0.88[d], −1.03(60)
1b	0.41(80), 0.84(80), 1.2[c]	−0.89[d], −1.07(50)
2a	0.44(100), 1.0(80)	−0.77(310)[e], −1.07
2b	0.40(80), 0.95(80)	−0.78(300)[e], −1.1[d]
3	1.04(80), 1.81(210)	−0.53[d], −0.80[d], −1.50[d], −1.77[d]
4a	0.96(100)[f], 1.14(100)[f]	−0.70(100), −1.01[d]
4b	0.93(100)[f], 1.09(80)[f]	−0.41[g], −0.67(90), −0.97[d]
5	1.03(60), 1.81(280)	−0.64[d], −0.87[d], −1.51[d], −1.79[d]

[a] Supporting electrolyte TBAP; reference electrode SCE; scanrate: 50 mV s^{-1}. [b] $E_{1/2} = 0.5(E_{pa} + E_{pc})$ where E_{pa} and E_{pc} are the anodic and cathodic peak potentials, respectively; $\Delta E_p = E_{pa} - E_{pc}$. [c] Irreversible, E_{pa}; a cathodic peak of unclear origin near 1.0 V appeared. [d] Irreversible, E_{pc}. [e] Quasi-reversible $i_{pc} > i_{pa}$. [f] Quasi-reversible, $i_{pa} > i_{pc}$. [g] Anodic responses generated *in situ* when the scan was allowed beyond −1.5 V.

electrochemically. Unfortunately, the oxidised complexes were not stable enough for their isolation, as they revert to the parent bivalent complexes rapidly. However, we were able to generate two representatives of the cationic complexes, *viz.* $[\mathbf{1a}]^+$ and $[\mathbf{2a}]^+$, in solution by the controlled potential bulk electrolysis of **1a** and **2a**.

In frozen (77 K) dichloromethane–toluene solutions the above low-spin osmium(III) (t_2^5) complexes displayed well-resolved rhombic spectra. The EPR data are collected in Table 3 and the spectra are shown in Fig. 5. The observed rhombicity of the EPR spectra in the present case[17] is understandable in terms of the gross molecular symmetry of these complexes, containing three non-equivalent axes. The rhombic distortion can be thought of as a combination of axial distortion (Δ, which splits t_2 into a and e) and rhombic distortion (V, which splits e). The splitting are illustrated as insets in Fig. 5. Spin-orbit coupling causes further changes in the energy gaps. Thus, two electronic transitions, of transition energies ΔE_1 and ΔE_2 ($\Delta E_1 < \Delta E_2$) are, in principle, probable within these three levels. All these energy parameters for the above low-spin osmium(III) complexes have been computed[18] using the observed g values. The axial distortion is indeed much stronger than the rhombic one. The analyses of EPR spectral data thus indicate that both $[\mathbf{1a}]^+$ and $[\mathbf{2a}]^+$ are significantly distorted from ideal octahedral arrangements, which indeed is in line with the observed structures of the parent bivalent complexes.

The voltammetric response of the pink dibromo compound $[Os(HL)(pap)Br_2]$, **4** consisted of two closely spaced quasi-reversible anodic responses near 0.9 and 1.1 V. A number of irreversible cathodic responses in the range −0.40 to −1.50 V were also observed. For comparison, the corresponding complex *cis*, *cis*-$Os(pap)_2Br_2$ undergoes two successive oxidations at 1.03 and 1.80 V, which are assigned to Os^{II}/Os^{III} and Os^{III}/Os^{IV} couples, respectively. The lowest potential anodic response near 0.9 V in **4** is thus assigned to a $Os^{II} \rightarrow Os^{III}$ couple occurring at the metal orbital (HOMO) and the second wave at 1.1 V is due[19] to ligand oxidation. Interestingly, the $E_{1/2}$ for the Os^{II}/Os^{III} response in **4** is similar to that in **5** but is far more anodic than those in **1** and **2**. The coordination of a hard amido donor function in the latter complexes is responsible for this cathodic shift.

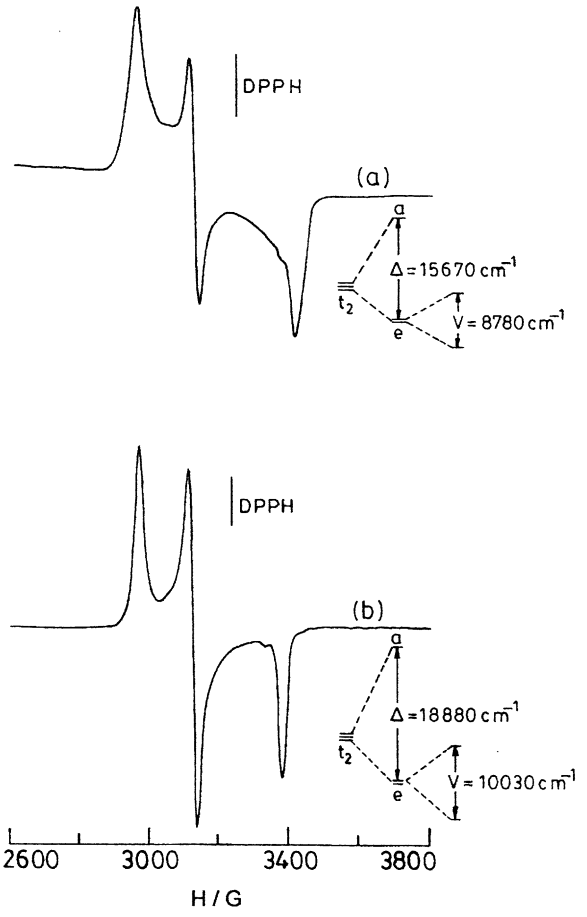

Fig. 5 EPR spectra of (a) $[Os(HL^a)(L^a)Br]^+$ and (b) $[Os(L^a)(pap)Br]^+$ in frozen 1 : 1 dichloromethane–toluene solution at 77 K, showing the computed splitting of the t_2 orbitals. DPPH = diphenylpicrylhydrazyl.

Table 3 EPR g values[a] and derived parameters[b] of the complexes $[\mathbf{1a}]^+$ and $[\mathbf{2a}]^+$

Derived energy parameters/cm^{-1}	Compd. $[\mathbf{1a}]^+$	$[\mathbf{2a}]^+$
g_1	2.2299	2.1862
g_2	2.0778	2.0743
g_3	1.8747	1.9165
Δ	15 670	18 880
V	8780	10 030
ΔE_1	11 625	14 125
ΔE_2	20 720	24 455

[a] In 1 : 1 dichloromethane–toluene solution at 77 K. [b] Taking the value of the spin-orbit coupling constant (λ) for low-spin osmium(III) as equal to 3000 cm^{-1}.

Conclusion

Our present study shows that the coordination chemistry of HL involving osmium(II) is rich with many novel features.

Osmium promoted deamination of HL has resulted in the formation of 2-(phenylazo)pyridine [pap], *in situ*, which is responsible for the several mixed ligand products that were formed from the reaction of $[NH_4]_2[OsBr_6]$ and HL. It may be noted here that the ligand HL is obtained[2] by amination of coordinated pap to a Co(II) centre. Both C–N bond formation and bond cleavage processes of the above kind are otherwise not achievable. Electronic reasons that govern the tridentate and bidentate coordination modes of the ligand have been noted. Presently we are pursuing the synthesis of monoaquo compounds from the monobromo compounds, **1** and **2**, by their hydrolysis. It is anticipated that these would be suitable mediators[20] for the study of oxo transfer processes.

Experimental

Materials and physical measurements

The starting compounds $[NH_4]_2[OsBr_6]$[21] and 2-[(arylamino)-phenylazo]pyridine[2] were prepared following the reported procedures.

Caution! Perchlorate salts of metal complexes can be explosive. Although no detonation tendencies have been observed, care is advised and handling of only small quantities recommended.

A Perkin–Elmer 240C elemental analyser was used to collect microanalytical data (CHN). The IR spectra were obtained with a Perkin–Elmer 783 spectrophotometer and the ^{1}H NMR spectra with a Bruker Avance DPX 300 spectrophotometer using $SiMe_4$ as an internal standard. Electrochemical measurements were performed at 298 K under a dry nitrogen atmosphere on a PC controlled PAR model 273A electrochemistry system. A platinum disc, a platinum wire auxiliary electrode and an aqueous saturated calomel reference electrode were used in a three-electrode configuration. The $E_{1/2}$ for the ferrocenium-ferrocene couple under our experimental conditions is 0.42 V. Electronic spectra were recorded on a JASCO V-570 spectrophotometer. EPR spectra were recorded on a Varian model 109C E-line X-band spectrometer fitted with a quartz Dewar for measurement at 77 K (liquid nitrogen) and all spectra were calibrated against the spectrum of DPPH.

Syntheses

The complexes **1**–**5** were isolated from the reaction of $[NH_4]_2[OsBr_6]$ with 2-[(arylamino)phenylazo]pyridine taken in a 1 : 2 molar ratio, in methanol, in the presence of dilute NEt_3. Details are given below.

Reaction of $[NH_4]_2[OsBr_6]$ with HL^a. A mixture of $[NH_4]_2[OsBr_6]$ (130 mg, 0.183 mmol), 2-[(arylamino)phenyl-azo]pyridine (100 mg, 0.365 mmol) and 2–3 drops of NEt_3 taken in 50 ml methanol was refluxed for 5 h on a steam bath. The initial red colour changed to dark brown during this period. The solution was cooled and concentrated to one-third of its initial volume and precipitated by the addition of diethyl ether. The crude product was then subjected to chromatography on a preparative TLC plate. It was first eluted with benzene; two brown bands (**1** and **2**) were separated. A small amount of unreacted ligand was observed at the junction of the two brown bands. The unmoved dark band was again loaded on a fresh preparative TLC plate and a benzene–chloroform mixture (3 : 1) was then used as the eluent. This resulted in the separation of three distinct bands, *viz*. violet (**3**), pink (**4**) and red-violet (**5**). All these compounds (**1**–**5**) were collected by the complete evaporation of eluates. Recrystallisation of these from a dichloromethane–hexane solvent mixture yielded the products in their crystalline states.

1a. Yield 18%, IR (KBr): $\nu = 3410$ (N–H), 1225, 1265 (N=N) cm^{-1}; calcd for $C_{34}H_{27}BrN_8Os$: C 49.94, H 3.33, N 13.70; found: C 49.79, H 3.06, N 13.40%. **2a.** Yield 22%, IR (KBr): $\nu = 1220$, 1265 (N=N) cm^{-1}; calcd for $C_{28}H_{22}BrN_7Os$: C 46.28, H 3.05, N 13.49; found: C 46.19, H 3.16, N 13.27%. **3.** Yield 5%, its spectra exactly corresponded to those of the known sample of *tc*-Os(pap)$_2$Br$_2$; calcd for $C_{22}H_{18}Br_2N_6Os$: C 36.88, H 2.53, N 11.73; found: C 35.61, H 2.34, N 11.12%. **4a.** Yield 10%, IR (KBr): $\nu = 3285$ (N–H), 1230, 1285 (N=N) cm^{-1}; calcd for $C_{28}H_{23}Br_2N_7Os$: C 41.64, H 2.87, N 12.14; found: C 41.52, H 2.91, N 12.18%. **5.** Yield 10%, its spectra exactly corresponded to those of the known sample of *cc*-Os(pap)$_2$Br$_2$; calcd for $C_{22}H_{18}Br_2N_6Os$: C 36.88, H 2.53, N 11.73; found: C 35.52, H 2.32, N 11.21%.

Reaction of $[NH_4]_2[OsBr_6]$ with HL^b. This reaction was performed as described above, except that an equivalent amount of HL^b was used in place of HL^a. The yields and characterisation data are given below.

1b. Yield 20%, IR (KBr): $\nu = 3410$ (N–H), 1220, 1265 (N=N) cm^{-1}; calcd for $C_{36}H_{31}BrN_8Os$: C 51.12, H 3.69, N 13.25; found: C 51.54, H 3.52, N 13.32%. **2b.** Yield 20%, IR (KBr): $\nu = 1220$, 1265 (N=N) cm^{-1}; calcd for $C_{29}H_{24}BrN_7Os$: C 47.03, H 3.27, N 13.24; found: C 46.85, H 3.26 N 13.13%. **4b.** Yield 12%, IR (KBr): $\nu = 3285$ (N–H), 1240, 1280 (N=N) cm^{-1}; calcd for $C_{29}H_{25}Br_2N_7Os$: C 42.40, H 3.07, N 11.93; found: C 42.28, H 3.02, N 11.81%. Yields of the compounds **3** and **5** were similar to those of the previous reaction.

Electrochemical generation of $[\mathbf{1a}]^+$ and $[\mathbf{2a}]^+$

The complexes $[\mathbf{1a}]^+$ and $[\mathbf{2a}]^+$ were generated in solution by constant potential coulometric oxidation of solutions of **1a** and **2a**, respectively. Details of a representative example are noted below.

A solution of 9.2 mg of **1a** in 25 ml dichloromethane solvent containing 35 mg of TBAP was oxidised coulometrically. The oxidation was performed at 0.65 V; $n = 1.108/1.086 = 1.02$, $n = Q/Q'$, where Q' is the calculated coulomb count for one electron transfer and Q is the coulomb count found after exhaustive electrolysis. A part of the electrogenerated solution (5 ml) of $[\mathbf{1a}]^+$ was mixed with an equal volume of toluene and the mixture was quickly frozen at 77 K, and then used for an EPR measurement. The oxidised complex $[\mathbf{1a}]^+$ was not stable at room temperature. Most of it (> 90%) underwent reduction to produce **1a**, associated with some insoluble material of unknown composition. The oxidation of **1a** also may be performed chemically using an aqueous solution of Ce^{4+}. In this case the quantity of the byproducts was more than 25%. To date, we were not successful in isolating the trivalent osmium compound $[\mathbf{1a}]^+$ in its pure state.

The trivalent complex $[\mathbf{2a}]^+$ was generated in solution similarly as described above.

Crystallography

X-Ray quality crystals of [Os(HL^a)(L^a)Br] (**1a**) were obtained by the slow diffusion of a dichloromethane solution of **1a** into hexane. Crystals of [Os(L^a)(pap)Br] (**2a**) were obtained by the slow diffusion of a solution of **2a** in toluene into hexane. Crystals of [Os(HL^a)(pap)Br$_2$](**4a**) were obtained by slow evaporation of a solution of **4a** in acetonitrile. Relevant crystallographic data are collected in Table 4. Intensity data of **1a** and **4a** were collected on a Siemens SMART diffractometer, equipped with a graphite-monochromated Mo-Kα radiation source, $\lambda = 0.71073$ Å. These were corrected for Lorentz-polarisation effects. The structures were solved by using the SHELXS-86 package of programmes[22] and refined by full-matrix least-squares based on F^2 (SHELXL-93).[23] All the

Table 4 Crystallographic data and refinement details of Os(HL^a)(L^a)Br (**1a**), Os(L^a)(pap)Br (**2a**) and Os(HL^a)(pap)Br$_2$ (**4a**)

	1a	**2a**	**4a**
Chemical formula	$C_{34}H_{27}BrN_8Os$	$C_{28}H_{22}BrN_7Os$	$C_{28}H_{23}Br_2N_7Os$
Formula weight	817.75	726.64	807.55
T/K	150(1)	295(2)	150(1)
Crystal system	Monoclinic	Monoclinic	Rhombohedral
Space group	$P2_1/n$	$P2_1/n$	$R\bar{3}$
a/Å	11.0940(2)	13.643(2)	38.4934(7)
b/Å	19.9527(3)	14.1915(18)	38.4934(7)
c/Å	14.5400(3)	13.850(3)	9.7379(2)
α/°	90	90	90
β/°	110.873(1)	91.36(2)	90
γ/°	90	90	120
u/Å^3	3007.28(9)	2680.8(8)	12 495.9(4)
Z	4	4	18
μ/mm^{-1}	5.608	6.278	7.501
Coll. reflect.	21 518	4731	24 176
Unique reflect.	6877	4731	6362
R_{int}	0.0264	0.0000	0.0445
R_1 $[I > 2\sigma(I)]$	0.0227	0.0353	0.0285
wR_2 $[I > 2\sigma(I)]$	0.0499	0.0650	0.0611

hydrogen atoms were located in calculated positions. The data of **2a** were collected on an Enraf-Nonius CAD4 diffractometer (Mo-Kα radiation, $\lambda = 0.71073$ Å) These were corrected for Lorentz-polarisation effects. The structure was solved by using the SHELXS-97 package of programmes[24] and refined by full-matrix least-squares based on F^2 (SHELXL-97).[25] Hydrogen atoms were added in the calculated positions.

CCDC reference numbers 157836–157838. See http://www.rsc.org/suppdata/nj/b1/b108507g/ for crystallographic data in CIF or other electronic format.

Acknowledgement

Financial support received from the Council of Scientific and Industrial Research, New Delhi, is acknowledged.

References

1 A. Saha, P. Majumdar, S.-M. Peng and S. Goswami, *Eur. J. Inorg. Chem.*, 2000, 2631.
2 A. Saha, P. Majumdar and S. Goswami, *J. Chem. Soc., Dalton Trans.*, 2000, 1703.
3 M. Okubo, C. Sugimori, M. Tokisada and T. Tsutsumi, *Bull. Chem. Soc. Jpn.*, 1986, **59**, 1644.
4 A. Saha, A. K. Ghosh, P. Majumdar, K. N. Mitra, S. Mondal, K. K. Rajak, L. R. Falvello and S. Goswami, *Organometallics*, 1999, **18**, 3772.
5 A. K. Ghosh, P. Majumdar, L. R. Falvello, G. Mostafa and S. Goswami, *Organometallics*, 1999, **18**, 5086.
6 (*a*) S. Goswami, R. N. Mukherjee and A. Chakravorty, *Inorg. Chem.*, 1983, **22**, 2825; (*b*) M. N. Ackermann, C. R. Batton, C. J. Deodene, E. M. Specht, S. C. Keill, W. E. Schreibet and H. Kim, *Inorg. Chem.*, 1989, **28**, 397; (*c*) J. J. Robertson, A. Kadziola, R. A. Krause and S. Larsen, *Inorg. Chem.*, 1989, **28**, 2097.
7 (*a*) A. K. Ghosh, S.-M. Peng, R. L. Paul, M. D. Ward and S. Goswami, *J. Chem. Soc., Dalton Trans.*, 2001, 336; (*b*) K. N. Mitra, P. Majumdar, S.-M. Peng, A. Castiñeiras and S. Goswami, *Chem. Commun.*, 1997, 1267; (*c*) K. N. Mitra, S.-M. Peng and S. Goswami, *Chem. Commun.*, 1998, 1685; (*d*) K. N. Mitra, S. Choudhury, A. Castiñeiras and S. Goswami, *J. Chem. Soc., Dalton Trans.*, 1998, 2901; (*e*) K. N. Mitra and S. Goswami, *Inorg. Chem.*, 1997, **36**, 1322.
8 (*a*) S. Bhattacharyya, T. J. R. Weakley and M. Chaudhury, *Inorg. Chem.*, 1999, **38**, 5453; (*b*) S. Bhattacharyya, T. J. R. Weakley and M. Chaudhury, *Inorg. Chem.*, 1999, **38**, 633; (*c*) S. D. Gray, K. J. Weller, M. A. Bruck, P. M. Briggs and D. E. Wigley, *J. Am. Chem. Soc.*, 1995, **117**, 10 678.
9 (*a*) A. Seal and S. Ray, *Acta Crystallogr., Sect. C*, 1984, **40**, 929; (*b*) K. Krause, R. A. Krause, S. Larsen and B. Rasmussen, *Acta Chem. Scand. Ser. A*, 1985, **39**, 375; (*c*) P. Majumdar, S.-M. Peng and S. Goswami, *J. Chem. Soc., Dalton Trans.*, 1998, 1569; (*d*) A. H. Velders, H. Kooijman, A. L. Spek, J. G. Haasnoot, D. de Vos and J. Reedijk, *Inorg. Chem.*, 2000, **39**, 2966.
10 B. K. Ghosh, A. Mukhopadhyay, S. Goswami, S. Ray and A. Chakravorty, *Inorg. Chem.*, 1984, **23**, 4633.
11 A. Saha, C. Das, S.-M. Peng and S. Goswami, *Indian J. Chem., Sect. A*, 2001, **40**, 198.
12 B. K. Ghosh, S. Goswami and A. Chakravorty, *Inorg. Chem.*, 1983, **22**, 3358.
13 (*a*) K. Tani, K. Nakajima, A. Iseki and T. Yamagata, *Chem. Commun.*, 2001, 1630; (*b*) K. Tani, A. Iseki and T. Yamagata, *Chem. Commun.*, 1999, 1821; (*c*) T. A. Smith and P. M. Maitlis, *J. Organomet. Chem.*, 1985, **289**, 385.
14 L. F. Warren, *Inorg. Chem.*, 1977, **16**, 2814.
15 C. Mealli and D. M. Proserpio, *J. Chem. Educ.*, 1990, **67**, 399.
16 (*a*) B. J. Pankuch, D. E. Lacky and G. A. Crosby, *J. Phys. Chem.*, 1980, **84**, 2061; (*b*) A. Ceulemans and L. G. Vanquickenborne, *J. Am. Chem. Soc.*, 1981, **103**, 2238; (*c*) S. Decurtins, F. Felix, J. Ferguson, H. U. Güdel and A. Ludi, *J. Am. Chem. Soc.*, 1980, **102**, 4102; (*d*) E. M. Kober and T. J. Meyer, *Inorg. Chem.*, 1982, **21**, 3967.
17 P. H. Rieger, *Coord. Chem. Rev.*, 1994, **135**/**136**, 203.
18 (*a*) B. Bleany and M. C. M. O'Brien, *Proc. Phys. Soc. London, Sect. B*, 1956, **69**, 1216; (*b*) J. S. Griffith, *The Theory of Transition Metal Ions*, Cambridge University Press, London, 1961, p. 363; (*c*) S. Bhattacharyya and A. Chakravorty, *Proc. Indian Acad. Sci., Chem. Sci.*, 1985, **95**, 159.
19 (*a*) G. M. Brown, T. R. Weaver, F. R. Keene and T. J. Meyer, *Inorg. Chem.*, 1976, **15**, 190; (*b*) F. R. Keene, D. J. Salmon and T. J. Meyer, *J. Am. Chem. Soc.*, 1976, **98**, 1884; (*c*) P. A. Adcock and F. R. Keene, *J. Am. Chem. Soc.*, 1981, **103**, 6494; (*d*) M. J. Ridd and F. R. Keene, *J. Am. Chem. Soc.*, 1981, **103**, 5733.
20 (*a*) S. Goswami, A. R. Chakravarty and A. Chakravorty, *J. Chem. Soc., Chem. Commun.*, 1982, 1288; (*b*) B. A. Moyer and T. J. Meyer, *Inorg. Chem.*, 1981, **20**, 436; (*c*) N. C. Pramanik, K. Pramanik, P. Ghosh and S. Bhattacharya, *Polyhrdron*, 1998, **17**, 1525; (*d*) R. R. Ruminski, S. Underwood, K. Vallely and S. J. Smith, *Inorg. Chem.*, 1998, **37**, 6528; (*e*) A. Gerli, J. Reedijk, M. T. Lakin and A. L. Spek, *Inorg. Chem.*, 1995, **34**, 1836.
21 F. P. Dwyer and J. W. Hogarth, *Inorg. Synth.*, 1957, **5**, 204.
22 G. M. Sheldrick, SHELXS86, Program for the Solution of Crystal Structures, University of Göttingen, Germany, 1990.
23 G. M. Sheldrick, SHELXL93, Program for the Refinement of Crystal Structures, University of Göttingen, Germany, 1993.
24 G. M. Sheldrick, *Acta Crystallogr., Sect. A*, 1990, **46**, 467.
25 G. M. Sheldrick, SHELXL97, Program for the Refinement of Crystal Structures, University of Göttingen, Germany, 1997.